Role of Vesicle-Associated Syntaxin 5 in the Assembly of Pre-Golgi Intermediates

Tony Rowe,* Christiane Dascher,* Sergei Bannykh, Helen Plutner, William E. Balch†

Syntaxins are thought to function during vesicular transport as receptors on the target membrane and to contribute to the specificity of membrane docking and fusion by interacting with vesicle-associated receptors. Here, syntaxin 5 (Syn5) was shown to be an integral component of endoplasmic reticulum–derived transport vesicles. This pool, but not the target, Golgi-associated Syn5 pool, was essential for the assembly of vesicular-tubular pre-Golgi intermediates and the delivery of cargo to the Golgi. The requirement for vesicle-associated Syn5 in transport suggests a reevaluation of the basis for operation of the early secretory pathway.

Syntaxin 5 is an essential membrane protein that mediates transport between the endoplasmic reticulum (ER) and Golgi (*1*, *2*). It belongs to the syntaxin family of SNAP-receptors (SNAREs), which are believed to function as target membrane receptors (t-SNAREs) that mediate docking with vesicle-associated receptors (v-SNAREs) of the synaptobrevin family (*3*, *4*). At steady state, Syn5 appears principally associated with the cis face of the Golgi (*1*, *5*, *6*). To determine whether its localization is dynamic, we took advantage of the observation that proteins recycling between the ER and Golgi preferentially accumulate in pre-Golgi intermediates when cells are incubated at reduced temperature (15°C) (*7*, *8*). Pre-Golgi intermediates consist of vesicular-tubular elements closely juxtaposed to ER export sites (*9*) that play a critical role in the recycling of transport components back to the ER (*10*, *11*). Recycling requires the COPI vesicle coat complex that is distinct from the COPII coat that drives export from the ER (*12*, *13*).

Incubation at 15°C led to a marked redistribution of Syn5 from the Golgi region at 32°C (Fig. 1, A and B) to pre-Golgi intermediates scattered throughout the peripheral cytoplasm (Fig. 1, C and D). The distribution of Syn5 at 15°C overlapped with that of p58 (Fig. 1D, inset), a molecule that actively recycles between the ER and Golgi (*7*, *10*, *11*), and vesicular stomatitis virus glycoprotein (VSV-G), a transmembrane cargo molecule that accumulates in pre-Golgi intermediates at 15°C (*10*) (Fig. 1C, inset). Furthermore, a mutant of the Sar1 guanosine triphosphatase, Sar1[GDP], which blocks COPII coat assembly and budding (*14*), caused the Golgi pool of Syn5 to redistribute to the ER like p58 (*10*, *15*). Thus, Syn5 appears to recycle rapidly between the ER and pre- or cis-Golgi compartments in a manner analogous to Syn1 in the synapse, which is present on both vesicles and the cell surface (*16*).

To examine the requirement for Syn5 in ER-to-Golgi transport in vitro, we added an affinity-purified Syn5-specific antibody prepared against the soluble cytoplasmic domain of Syn5 [Syn5-11 (*17*)] to an assay that reconstitutes the transport of VSV-G in permeabilized cells (*18*, *19*). The antibody recognized both 42- and 35-kD isoforms (*20*, *21*) of Syn5 on immune blots of whole-cell extracts (*15*). The intact antibody or Fab fragments inhibited ER–to–cis-Golgi transport in a dose-dependent manner as measured by acquisition of sensitivity to endoglycosidase D (endo D) (Fig. 2A). Addition of a soluble cytoplasmic domain fragment of Syn5 (Syn5-11) (*1*) also partially inhibited transport (Fig. 2B), consistent with its effects in vivo (*1*). Inhibition of transport by the antibody to Syn5 (anti-Syn5) was specific as it was blocked by preneutralization with Syn5-11 (Fig. 2A, inset).

The ability of Syn5-specific reagents to inhibit ER-to-Golgi transport in permeabilized cells could reflect either inhibition of vesicle formation or their delivery to pre- or cis-Golgi compartments or both. To distinguish between these possibilities, we used a microsome-based assay that reconstitutes the formation of COPII-coated, ER-derived vesicles (*14*). This assay uses differential centrifugation to separate the slowly sedimenting ER-derived vesicles released into the medium speed supernatant (MSS) from the rapidly sedimenting ER and Golgi membranes that are recovered in the medium speed pellet (MSP). Anti-Syn5 had no effect on the appearance of VSV-G in the MSS, in contrast to a control reaction containing Sar1[GDP], which blocked the formation of VSV-G–containing vesicles (*14*) (Fig. 2C). Thus, ER-derived vesicle formation does not require Syn5 function.

Because Syn5 recycled between the ER

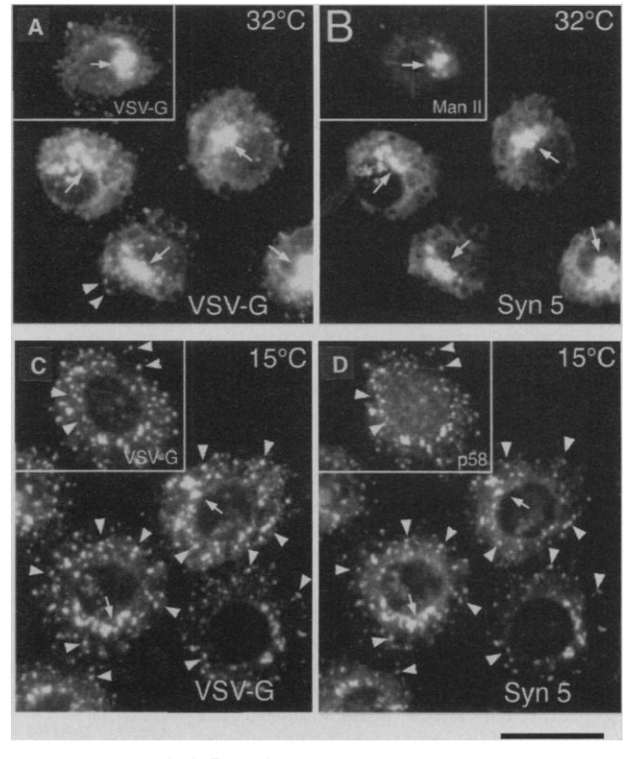

Fig. 1. Syn5 recycles between the ER and Golgi compartments. The distribution of Syn5 in vivo was examined by indirect immunofluorescence after incubation of NRK cells either at 32°C (**A** and **B**) or 15°C (60 min) (**C** and **D**) (*43*). Cells were infected with the tsO45 strain of vesicular stomatitis virus at the restrictive temperature (39.5°C) to accumulate VSV-G in the ER, before the temperature shift. Upon shift to 32°C, Syn5 overlapped with VSV-G and the Golgi marker α-1,2 mannosidase II (Man II) [arrows in (A) to (D), insets]. At 15°C, Syn5 accumulated in pre-Golgi intermediates as indicated by its overlap with VSV-G and p58 [arrowheads in (A) to (D), insets]. This accumulation could be detected as early as 15 min after shift to 15°C (not shown). No change in the distribution of the Golgi processing enzyme α-1,2-mannosidase II was observed under these conditions (*15*). Bar: 20 μm.

Department of Cell Biology, The Scripps Research Institute, 10550 North Torrey Pines Road, La Jolla, CA 92037, USA.

*These authors contributed equally to this work.
†To whom correspondence should be addressed. E-mail: webalch@scripps.edu

and Golgi (Fig. 1), we tested whether it was a component of ER-derived vesicles. We prepared affinity-purified vesicles using an antibody specific for the cytoplasmic tail of VSV-G (*14*) and examined their composition by immune blotting. The ER-derived vesicles generated under normal incubation conditions contained Syn5 and its interacting protein, Sly1, along with VSV-G and p58 (Fig. 3A, lane b), and the vesicles contained the mammalian ER-to-Golgi v-SNAREs mSec22b, membrin, and rBet1 (*20*) (Fig. 3B, lane b). In controls, the levels of these proteins recovered on beads were reduced (>90%) when anti–VSV-G was omitted from the immunoisolation procedure (Fig. 3, A and B, lane a) or when COPII vesicle formation was blocked with Sar1[GDP] (Fig. 3, A, lane c, and B, lane d). Incubation in the presence of anti-Syn5 (Fig. 3A, lane d) or Fab fragments (Fig. 3A, lane e) blocked the incorporation of both Syn5 and Sly1 into vesicles without affecting the recovery of VSV-G and p58. In contrast to the almost complete (>99%) removal of Syn5 from vesicles in the presence of anti-Syn5, the recovery of membrin was only partially reduced (~50%), and rBet1 and mSec22b were unaffected (Fig. 3B). Thus, vesicles generated in the presence of antibody were not depleted of v-SNARES, providing us with a test for the role of vesicle-associated Syn5 in ER-to-Golgi transport.

According to the SNARE hypothesis, the interaction of syntaxins with their cognate v-SNAREs upon vesicle docking generates a 7*S* complex and leads to the binding of *N*-ethyl-maleimide–sensitive factor (NSF) and SNAPs and the formation of a transient 20*S* SNARE complex (*22*). More recent studies, however, suggest that NSF function is complete before vesicle docking (*23*) and that SNARE complexes can assemble on purified synaptic vesicles (*16*, *24*) and clathrin-coated vesicles (*25*). To test whether Syn5 could participate in SNARE complex assembly on undocked ER-derived vesicles, we prepared detergent extracts of affinity-purified COPII vesicles and incubated them in the absence or presence of Myc-tagged NSF (Myc-NSF) and α-SNAP. In control incubations lacking Myc-NSF, Syn5 was not immunoprecipitated with anti-Myc (Fig. 3C, lane a) and sedimented as a 5*S* to 7*S* complex (Fig. 3D, upper panel). Under conditions that promote the stable assembly of 20*S* complexes [by preventing adenosine triphosphate (ATP) hydrolysis by NSF], Syn5 (20 to 25% of total) coimmunoprecipitated with NSF (Fig. 3C, lane b) and sedimented as a ~20*S* particle (Fig. 3D, middle panel). The interaction of Syn5 with NSF was blocked in the presence of the anti-Syn5 Fab fragment, but not a control Fab (Fig. 3C, lanes c and d). Immunoprecipitation with anti-

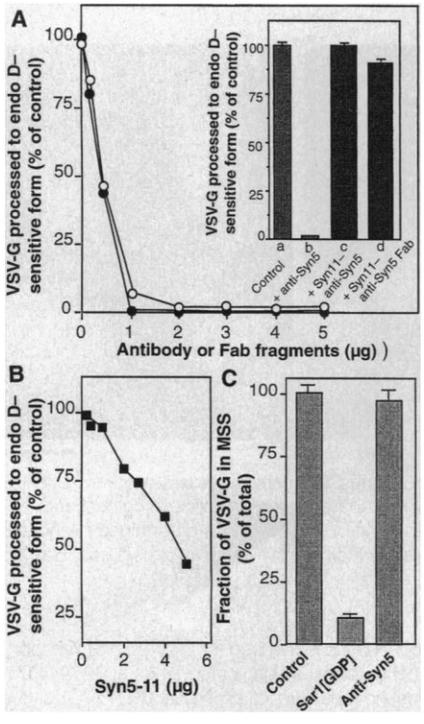

Fig. 2. Syn5 is required for ER-to-Golgi transport at a downstream vesicle targeting or fusion step. Anti-Syn5 or its Fab fragments (**A**) or Syn5-11 (**B**) were added to semi-intact cell transport assays (*44*) at the concentrations indicated. Transport was followed by measuring the conversion of VSV-G to the endoglycosidase D (endo D)–sensitive cis Golgi form. (A, inset) The assay was either not supplemented (lane a), or supplemented with 1 μg of anti-Syn5 alone (lane b) or 1 μg of anti-Syn5 (lane c) or Fab (lane d) pre-neutralized with Syn5-11 (1 μg). The amounts of VSV-G processed are reported relative to untreated controls in which ~80% of total VSV-G was transported. (**C**) Microsomes were incubated for 5 min at 32°C in the absence or presence of either 1 μg of Sar1[GDP] (*14*) or 1 μg of anti-Syn5 (*45*). The relative amounts of ER-derived vesicles released into the MSS were determined by quantitative immune blotting for VSV-G (*45*). Mean values of duplicate samples are shown with the indicated error range.

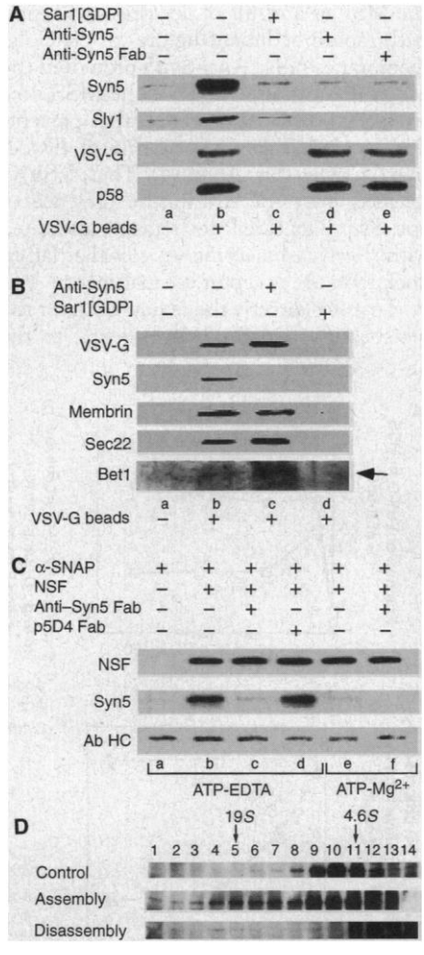

Fig. 3. Syn5 can assemble into a 20*S* SNARE complex on free ER-derived vesicles. (**A** and **B**) ER-derived vesicles were immunoisolated on magnetic beads with the use of an antibody against the cytoplasmic tail of VSV-G (*14*, *45*). The vesicles were solubilized in gel sample buffer and analyzed by immune blotting for Syn5, Sly1, VSV-G, p58, and the v-SNAREs mSec22b, rBet1, and membrin (*20*) as indicated. The 35- and 42-kD isoforms of Syn5 were detected with roughly equal intensity. The 42-kD isoform is shown. The vesicle formation reactions were either not supplemented (A and B, lanes a and b), or supplemented with 2.5 μg of Sar1[GDP] (A, lane c; B, lane d), anti-Syn5, (A, lane d; B, lane c), or Fab (A, lane e). The amount of Syn5 recovered on the vesicles in lane b represented 4 to 5% of the total Syn5 present in the microsome fraction. This corresponds to the recovery of recycling p58 (~5%) (*14*) and reflects both the efficiency of vesicle formation in vitro and the immunoisolation procedure. (**C**) The ability of Syn5 on affinity-purified ER-derived vesicles to interact with Myc-tagged NSF as measured by coimmunoprecipitation (*46*). Detergent extracts of the vesicles were incubated under 20*S* complex assembly (lanes a to d) or disassembly (lanes e and f) conditions in the presence of recombinant α-SNAP and magnetic bead–anti-Myc conjugates alone (lane a) or pre-bound to Myc-NSF (lanes b to f). The incubations were supplemented with the anti-Syn5 Fab (lanes c and f) or a control Fab (lane d). The recoveries of NSF, Syn5, and anti-Myc heavy chain (Ab HC) were measured by SDS-PAGE analysis of the washed immunoprecipitates followed by immune blotting. (**D**) Glycerol density gradient analysis of Syn5 present on affinity-purified vesicles. Detergent extracts of the vesicles were incubated under assembly or disassembly conditions in the presence of recombinant α-SNAP and Myc-NSF (*46*). The control was incubated under assembly conditions in the absence of NSF and SNAP. The reactions were run on linear glycerol density gradients then fractionated (lanes 1 to 14). The fractions were precipitated, then analyzed by SDS-PAGE followed by immune blotting for Syn5. The location of 4.6*S* (albumin) and 19*S* (α_2-macroglobulin) are indicated by arrows.

Syn5 showed that Syn5 was associated with membrin in both the 7S and 20S complexes (*15*) as demonstrated previously (*20*). mSec22B and rBet1 are also likely to be components of these complexes because interactions between Syn5 and these v-SNAREs and their yeast homologs are well documented (*20*, *26*–*28*). Under disassembly conditions (supporting ATP hydrolysis by NSF), Syn5 (Fig. 3C, lane e) was not recovered in the anti-Myc immunoprecipitate and association with membrin was lost (*15*). Accordingly, the 20S pool of Syn5 shifted to a low molecular weight form (Fig. 3D, lower panel), reflecting complete dissolution of the 20S complex as observed previously (*20*, *22*). Thus, ER-derived vesicles can support formation of a 20S complex before vesicle docking.

To determine whether Syn5 is required for vesicle docking, we supplemented the microsome-based assay with anti-Syn5 and monitored the levels of VSV-G in the MSS with increasing time of incubation. Vesicles released from sedimentable ER membranes during the first 10 to 15 min of incubation are subsequently redirected to the MSP as a result of docking and fusion with rapidly sedimenting pre- or cis-Golgi membranes (*14*). Anti-Syn5 promoted the accumulation of VSV-G in the MSS, like Sar1[GTP], a mutant protein that prevents docking by blocking uncoating of ER-derived vesicles (Fig. 4A) (*14*). Thus, VSV-G released from the ER in the presence of anti-Syn5 appeared to remain associated with slowly sedimenting vesicles that fail to dock with the acceptor compartment.

To assess directly the requirement for the vesicular pool of Syn5 in targeting to the cis-Golgi compartment, we monitored VSV-G transport using a two-stage assay (*14*). In this assay, ER-derived vesicles released into the MSS during stage 1 were washed and reincubated in the presence of cytosol, ATP, and purified acceptor Golgi membranes (stage 2). When anti-Syn5 was added only to stage 1, the resulting Syn5-depleted vesicles were unable to deliver VSV-G to the cis-Golgi compartment in stage 2 efficiently (Fig. 4B, lane c). Inhibition was neutralized by preincubation of anti-Syn5 with Syn5-11 (Fig. 4B, lane d). No inhibition was observed when the vesicles were generated in the presence of a control antibody specific for Syn1 (Fig. 4B, lane e). Inhibition was also observed when vesicles produced in stage 1 were isolated, pretreated with anti-Syn5 Fab, and reincubated in the absence of antibody in stage 2; parallel incubation with a control Fab recognizing the cytoplasmic tail of VSV-G had no effect (*15*). Thus, the vesicle-associated pool of Syn5 is required for delivery of cargo to the cis-Golgi.

To analyze the role of Syn5 in vesicle targeting or fusion further, we incubated vesicles formed in stage 1 reactions lacking antibody with acceptor Golgi in the presence of anti-Syn5 in stage 2. Inhibition was again observed (Fig. 4B, lane f), and preincubation with Syn5-11 neutralized the inhibition (Fig. 4B, lane g). The transport block could reflect inhibition of the Syn5 pool associated either with ER-derived vesicles or that which is present on the acceptor compartment or

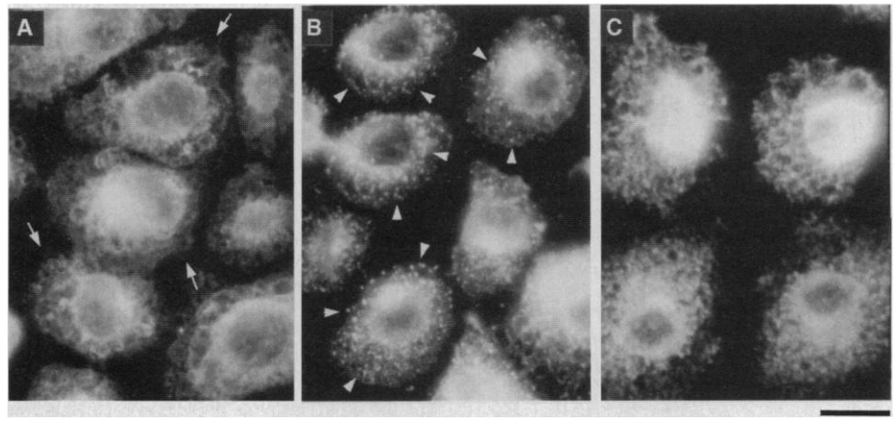

Fig. 5. Syn5 is required for assembly of pre-Golgi intermediates. Permeabilized cells containing VSV-G in the ER (*30*) were prepared and either held on ice (**A**) or incubated in the presence of cytosol and ATP in the absence (**B**) or presence of anti-Syn5 (**C**). The distribution of VSV-G was determined by indirect immunofluorescence (*43*). Arrows indicate ER; arrowheads indicate pre-Golgi intermediates. Bar: 20 μm.

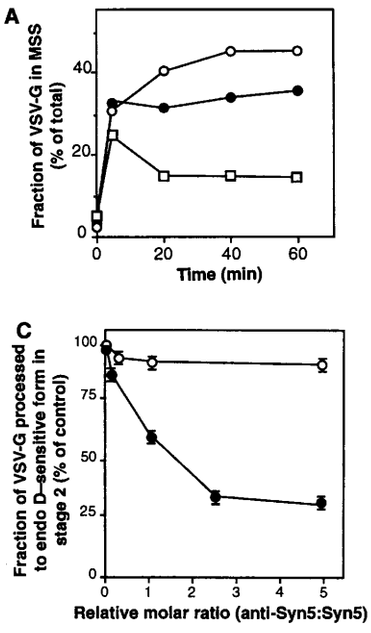

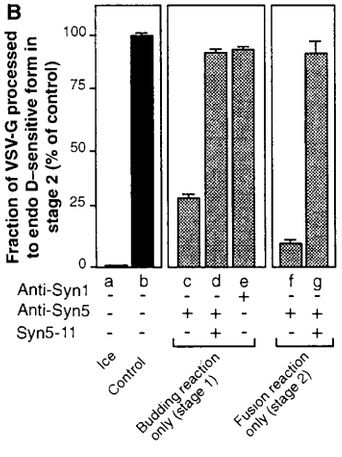

Fig. 4. The vesicular pool of Syn5 is required for ER-to-Golgi transport. (**A**) Microsomes were incubated for the indicated times at 32°C (*45*) in the absence (□) or presence of 1 μg of either Sar1[GTP] (○) or the Syn5-specific antibody (●). The levels of ER-derived vesicles recovered in the MSS were quantitated by immune blotting for VSV-G. (**B**) Two-stage vesicle consumption assays (*45*). Control incubations (lanes a and b) in which microsomes were incubated for 10 min at 32°C, then either maintained on ice (lane a) or incubated for 60 min in stage 2 with acceptor Golgi membranes (*45*) (lane b). The amount of VSV-G processed to the endo D–sensitive form was determined. Lanes c to e: Stage 1 incubations were performed in the presence of anti-Syn5 alone (2.5 μg) (lane c) or anti-Syn1 (2.5 μg) (lane e), or anti-Syn5 pre-neutralized with Syn5-11 (lane d). Lanes f and g: Vesicles generated in the absence of antibody in stage 1 were recovered in the MSS, washed, and reincubated in stage 2 (60 min, 32°C) in the presence of acceptor Golgi membranes (*47*) and either anti-Syn5 alone (5 μg) (lane f) or pre-neutralized with Syn5-11 (lane g). (**C**) (●) Vesicles synthesized in the presence of anti-Syn5 in stage 1 were incubated in the absence of antibody in stage 2. (○) Golgi membranes (*47*) were pretreated with anti-Syn5, then neutralized with Syn5-11 before stage 2 incubations containing vesicles generated in stage 1 in the absence of antibody. The amounts of anti-Syn5 used for pretreatment of either the microsomes in stage 1 or the Golgi before stage 2 were adjusted to obtain equivalent molar ratios of antibody to total Syn5 protein (35- and 42-kD isoforms). The amounts of VSV-G processed are reported relative to untreated controls in which ~30% of total VSV-G was transported. Mean values of duplicate samples are shown with the indicated error range.

both. Therefore, we preincubated the Golgi membranes with anti-Syn5 at molar ratios (anti-Syn5:protein) that were inhibitory when added to stage 1 incubations. Before incubation in stage 2, the antibody was neutralized with Syn5-11 at concentrations sufficient to bind excess antibody, but not to interfere with transport. Fusion was only marginally (<10%) inhibited compared with the 70 to 75% block observed when Syn5-depleted vesicles were added to untreated Golgi membranes (Fig. 4C). In immunoprecipitation experiments, the Golgi membrane–associated Syn5 pool, like the ER pool, was fully accessible to antibody under standard transport reaction conditions (*15*). Addition of Syn5-11 to antibody-treated microsomes before stage 1 incubations at 32°C did not abolish inhibition of transport, indicating that Syn5-11 did not dissociate the antibody from membranes (*15*). Thus, we could not demonstrate a requirement for the cis-Golgi pool of Syn5 in transport.

Because vesicle-associated Syn5 was required for ER-to-Golgi transport, we investigated whether it participates in the assembly of pre-Golgi intermediates in vitro. Incubation in the presence of cytosol and ATP for 15 min at 32°C leads to transport of VSV-G from the ER (Fig. 5A) into numerous punctate pre-Golgi intermediates (Fig. 5B) before delivery to the Golgi at later time points (*19*, *29*, *30*). Anti-Syn5 (Fig. 5C) or Fab fragments (*15*) inhibited the appearance of VSV-G–containing intermediates. This was confirmed by electron microscopy in combination with quantitative morphometry (*9*). Whereas intermediates were readily detected in control incubations (676 detected in ~40 cells), they were largely undetectable in permeabilized cells incubated in the presence of anti-Syn5 (<5% of control value in ~400 cells). Because vesicle budding from the ER was unaffected by the antibody (Fig. 2), it was apparent that vesicles released from the ER in permeabilized cells failed to coalesce into detectable pre-Golgi intermediates in the absence of Syn5 function.

The requirement for a functional syntaxin family member on ER-derived vesicles is supported by evidence demonstrating that SNARE complexes form on other vesicular carriers (*16*, *25*) and, in the case of synaptic vesicles, that Syn1 is the target for inactivation by the botulinin C1 toxin (*24*). It is now apparent that it may be difficult to predict the function of syntaxins from their steady-state morphological distributions. Several lines of evidence now demonstrate that the transient formation of a 20S intermediate mediated by NSF and SNAPS may promote the disassembly of syntaxins from the SNARE complex, thereby priming membranes for subsequent docking and fusion (*23*, *31*–*34*). Our results are consistent with these observations. Thus, activation of vesicle-associated syntaxin may be a more general feature of vesicular traffic than previously anticipated.

The demonstration that Syn5 functions on ER-derived vesicles provides insight into the functional basis for operation of the early secretory pathway. Instead of ER-to-Golgi transport being mediated directly by COPII vesicles as suggested by studies in yeast (*35*), our data now provide biochemical evidence that Syn5 may be required for the fusion of COPII vesicles to generate tubular elements of pre-Golgi intermediates. This conclusion is consistent with the ability of intermediates to form de novo in the cell periphery to collect cargo molecules such as VSV-G (*9*, *36*) and move en bloc in a microtubule-dependent manner to the Golgi complex (*7*, *36*). The role for Syn5 in pre-Golgi intermediate formation may be analogous to the syntaxin requirement in yeast homotypic vacuole fusion (*31*). That the generation of tubular recycling intermediates requires Syn5 function and is critical for transport is consistent with the possibility that their assembly to form the cis-Golgi network (*36*) provides the foundation for the subsequent maturation of the Golgi (*37*).

REFERENCES AND NOTES

1. C. Dascher, J. Matteson, W. E. Balch, *J. Biol. Chem.* **269**, 29363 (1994).
2. K. G. Hardwick and H. R. B. Pelham, *J. Cell Biol.* **119**, 513 (1993).
3. T. Söllner, M. K. Bennett, S. W. Whiteheart, R. H. Scheller, J. E. Rothman, *Cell* **75**, 409 (1993).
4. M. K. Bennett and R. H. Scheller, *Proc. Natl. Acad. Sci. U.S.A.* **90**, 2559 (1993).
5. M. K. Bennett *et al.*, *Cell* **74**, 863 (1993).
6. D. K. Banfield, M. J. Lewis, C. Rabouille, G. Warren, H. R. B. Pelham, *J. Cell Biol.* **127**, 357 (1994).
7. J. Saraste and K. Svensson, *J. Cell Sci.* **100**, 415 (1991).
8. J. Saraste and E. Kuismanen, *Cell* **38**, 535 (1984).
9. S. I. Bannykh, T. Rowe, W. E. Balch, *J. Cell Biol.* **135**, 19 (1996).
10. M. Aridor, S. I. Bannykh, T. Rowe, W. E. Balch, *ibid.* **131**, 875 (1995).
11. B. L. Tang, S. H. Low, H.-P. Hauri, W. Hong, *Eur. J. Cell Biol.* **68**, 397 (1995).
12. R. Schekman and L. Orci, *Science* **271**, 1526 (1996).
13. J. E. Rothman and F. Wieland, *ibid.* **272**, 227 (1996).
14. T. Rowe, M. Aridor, J. M. McCaffery, H. Plutner, W. E. Balch, *J. Cell Biol.* **135**, 895 (1996).
15. T. Rowe and W. E. Balch, unpublished results.
16. C. Walch-Solimena *et al.*, *J. Cell Biol.* **128**, 637 (1995).
17. C. Dascher and W. E. Balch, *J. Biol. Chem.* **271**, 15866 (1996).
18. C. J. M. Beckers, D. S. Keller, W. E. Balch, *Cell* **50**, 523 (1987).
19. H. W. Davidson and W. E. Balch, *J. Biol. Chem.* **268**, 4216 (1993).
20. J. C. Hay, D. S. Chao, C. S. Kuo, R. H. Scheller, *Cell* **89**, 149 (1997).
21. N. Hui *et al.*, *Mol. Biol. Cell* **8**, 1777 (1997).
22. T. Söllner *et al.*, *Nature* **362**, 318 (1993).
23. A. Mayer, W. Wickner, A. Haas, *Cell* **85**, 83 (1996).
24. H. Otto, P. I. Hanson, R. Jahn, *Proc. Natl. Acad. Sci. U.S.A.* **94**, 6197 (1997).
25. G. J. Steel, M. Tagaya, P. G. Woodman, *EMBO J.* **15**, 745 (1996).
26. M. Sacher, S. Stone, S. Ferro-Novick, *J. Biol. Chem.* **272**, 17134 (1997).
27. J. P. Lian, S. Stone, Y. Jiang, P. Lyons, S. Ferro-Novick, *Nature* **372**, 698 (1994).
28. M. Sögaard *et al.*, *Cell* **78**, 937 (1994).
29. W. E. Balch, J. M. McCaffery, H. Plutner, M. G. Farquhar, *ibid.* **76**, 841 (1994).
30. H. Plutner, H. W. Davidson, J. Saraste, W. E. Balch, *J. Cell Biol.* **119**, 1097 (1992).
31. B. J. Nichols, C. Ungermann, H. R. B. Pelham, T. Wickner, A. Haas, *Nature* **387**, 199 (1997).
32. L. H. Chamberlain, D. Roth, A. Morgan, R. D. Burgoyne, *J. Cell Biol.* **130**, 1063 (1995).
33. A. Banerjee, V. A. Barry, B. R. DasGupta, T. F. J. Martin, *J. Biol. Chem.* **271**, 20223 (1996).
34. P. I. Hanson, R. Roth, H. Morisaki, R. Jahn, J. E. Heuser, *Cell* **90**, 523 (1997).
35. C. Barlowe *et al.*, *ibid.* **77**, 895 (1994).
36. J. F. Presley *et al.*, *Nature* **389**, 81 (1997).
37. S. Bannykh and W. E. Balch, *J. Cell Biol.* **138**, 1 (1997).
38. T. E. Kreis, *EMBO J.* **5**, 931 (1986).
39. A. Velasco *et al.*, *J. Cell Biol.* **122**, 39 (1993).
40. D. W. Wilson, S. W. Whiteheart, M. Wiedmann, M. Brunner, J. E. Rothman, *ibid.* **117**, 531 (1992).
41. S. Fleischer and M. Kervina, *Methods Enzymol.* **31**, 6 (1974).
42. V. Malhotra, T. Serafini, L. Orci, J. C. Shepherd, J. E. Rothman, *Cell* **58**, 329 (1989).
43. NRK cells on cover slips were infected at the restrictive temperature (39.5°C) with the tsO45 strain of VSV (*30*). The cells were subsequently shifted to either 15° or 32°C, then permeabilized with digitonin and probed with the appropriate primary antibodies followed by fluorescently labeled secondary antibodies (*30*). The primary antibodies used were directed against Syn5 (*17*), VSV-G (p5D4) (*38*), and α-1,2-mannosidase II (*39*).
44. NRK cells were infected with tsO45 VSV for 4 hours at 39.5°C, then transferred to ice and permeabilized (*18*). Transport reactions containing semi-intact cells, gel-filtered cytosol, ATP mix, and uridine 5′-triphosphate–*N*-acetylglucosamine were performed for 60 min at 32°C and the membranes subsequently digested with endo D and β-*N*-acetylglucosaminidase (*19*). Syntaxin 5–specific reagents were preincubated in complete reaction cocktails on ice for 20 min before transfer to 32°C. Processing of VSV-G to the endo D–sensitive form was followed by quantitative immune blotting (*14*).
45. Vesicle formation and two-stage assays were done as described (*14*) with the following modifications: (i) The membranes were resuspended in 0.25 M sucrose, 10 mM Hepes (pH 7.4) before the addition of salts and differential centrifugation; (ii) the medium speed spin was increased to 5 min in the two-stage assay; and (iii) stage 2 incubations contained gel-filtered cytosol (*19*). Endo D digestion was performed as described above.
46. Immunoisolated ER-derived vesicles (*14*) were solubilized in 0.5% Triton X-100 buffers containing either ATP and EDTA (assembly) or MgATP (disassembly) (*22*). For immunoprecipitation experiments, the vesicle extracts (0.4 ml) were incubated with 0.5 mg of α-SNAP and Myc-NSF immobilized on anti-Myc–coupled magnetic beads. The immunoprecipitates were washed extensively before SDS–polyacrylamide gel electrophoresis (PAGE) and immune blotting. Analysis on 10 to 40% (w/v) glycerol density gradients was done as described (*40*). Fractions were collected and precipitated with 10% trichloroacetic acid before SDS-PAGE and immune blotting with enhanced chemiluminescence detection.
47. Rat livers (20 g) were excised and placed in 100 ml of 0.5 M sucrose, 5 mM EDTA, 5 mM EGTA, 10 mM tris-HCl (pH 7.4) supplemented with a protease inhibitor cocktail (PIC) (*14*). The tissue was homogenized (*41*) and the homogenate centrifuged at 800*g* for 10 min. The Golgi membranes were isolated from the postnuclear supernatant fraction by

ultracentrifugation on sucrose density gradients (*42*). The Golgi fraction was collected, diluted with 4 volumes of 87.5 mM KOAc, 1.25 mM $Mg(OAc)_2$, and 20 mM Hepes (pH 7.4) and sedimented at 16,000*g* for 10 min. The membrane pellet was washed with transport buffer [0.25 M sorbitol, 70 mM KOAc, 1 mM $Mg(OAc)_2$, 20 mM Hepes (pH 7.4)], then resuspended in 4 ml of transport buffer plus PIC. The Golgi membranes were divided into 0.1-ml samples, frozen in liquid nitrogen, and stored at −80°C.

48. We thank R. Scheller and J. Hay (Stanford University) for antibodies to mSec22b, rBet1, and membrin; J. Saraste (University of Bergen, Bergen, Norway) for anti-p58; and S. Whiteheart (University of Kentucky Medical Center) for recombinant α-SNAP, Myc-tagged NSF, and anti-NSF (6E6). Supported by NIH grant GM 42336 (to W.E.B.) and the National Cancer Institute (CA58689). Electron microscopy made extensive use of Core B in CA58689. T.R. is a recipient of a fellowship from the Muscular Dystrophy Association, C.D. is a recipient of a fellowship grant from the Deutsche Forschungsgemeinschaft, and S.B. is a recipient of a Cystic Fibrosis Foundation Fellowship.

14 October 1997; accepted 28 November 1997

Differential Use of CREB Binding Protein–Coactivator Complexes

Riki Kurokawa, Daniel Kalafus, Marie-Hélène Ogliastro, Chrissa Kioussi, Lan Xu, Joseph Torchia, Michael G. Rosenfeld, Christopher K. Glass

CREB binding protein (CBP) functions as an essential coactivator of transcription factors that are inhibited by the adenovirus early gene product E1A. Transcriptional activation by the signal transducer and activator of transcription–1 (STAT1) protein requires the C/H3 domain in CBP, which is the primary target of E1A inhibition. Here it was found that the C/H3 domain is not required for retinoic acid receptor (RAR) function, nor is it involved in E1A inhibition. Instead, E1A inhibits RAR function by preventing the assembly of CBP–nuclear receptor coactivator complexes, revealing differences in required CBP domains for transcriptional activation by RAR and STAT1.

Analysis of the mechanisms by which the adenovirus E1A oncoprotein inhibits cellular differentiation and promotes dysregulated growth has contributed to the identification and functional characterization of cellular regulatory proteins that include Rb, p107, CBP, and p300 (*1*, *2*). CBP and the related p300 function as coactivator proteins for several transcription factors, including CREB (cyclic AMP response element–binding protein) (*3*), AP-1 (*4*), nuclear receptors (*5*), and STAT proteins (*6*). CBP and p300 interact with regulatory proteins through a series of conserved domains (Fig. 1A), with the cysteine-histidine–rich region (C/H3) (*2*) mediating direct interactions with E1A, STAT1, cFos, p/CAF, and RNA helicase A (*4*, *6*–*8*). Although E1A may inhibit the activities of cFos and STAT1 by competing for this interface, other transcription factors that are inhibited by E1A, such as CREB and nuclear receptors, do not interact with this region. E1A inhibits CREB function by preventing the association of a complex of RNA polymerase II and RNA helicase A with the C/H3-E1A interaction domain (*8*). These observations raise the questions of whether recruitment of complexes containing RNA polymerase II to the C/H3-E1A binding site is a general requirement for CBP and p300 to function as transcriptional coactivators and whether competition for this interaction accounts for the inhibitory effects of E1A on other CBP- and p300-dependent factors such as nuclear receptors.

We compared the ability of E1A to inhibit CBP-stimulated transcriptional activation by RARs and STAT1 (*9*). Complete inhibition of RAR activity required about 10 times the amount of E1A than was required for STAT1, suggesting differential use of the C/H3 domain (Fig. 1B). We therefore examined the ability of wild-type CBP and a CBP mutant lacking the C/H3 domain (CBPΔC/H3) to serve as coactivators of RAR and STAT1. Overexpression of wild-type CBP potentiated STAT1-dependent transcription, whereas CBPΔC/H3 was inactive (Fig. 1B). However, CBPΔC/H3 was nearly as effective as wild-type CBP in stimulating RAR activity (Fig. 1B), indicating that the C/H3 domain is not required for CBP to serve as a coactivator of RAR.

We tested the ability of E1A to inhibit the stimulatory effects of CBPΔC/H3 on RAR-dependent transcription. E1A was as effective in inhibiting the coactivator function of CBPΔC/H3 as it was in inhibiting wild-type CBP (Fig. 2A), and glutathione S-transferase (GST)–E1A fusion proteins interacted with CBPΔC/H3 almost as effectively as with wild-type CBP [Fig. 2B and

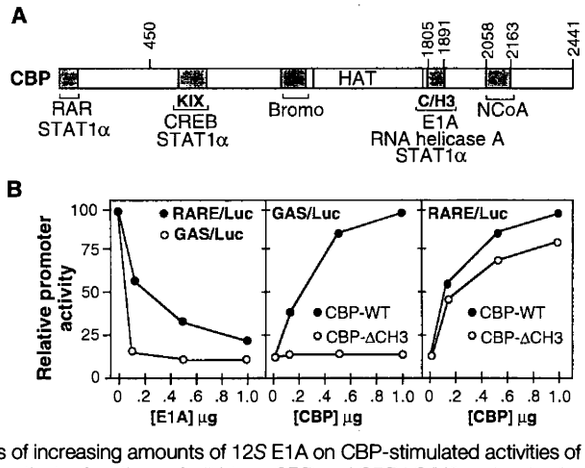

Fig. 1. The retinoic acid receptor (RAR) and STAT1 exhibit differential requirements for the C/H3 domain of CBP. (**A**) CBP interaction domains. The KIX (kinase-inducible interaction) domain mediates interactions with phosphorylated CREB and STAT1. C/H3 is a cysteine-histidine–rich region that mediates interactions with several factors, including E1A, STAT1, and complexes of RNA helicase A and RNA polymerase II. The region in CBP that interacts with nuclear receptor coactivators is indicated as NCoA. Numbers above CBP indicate endpoints of CBP deletion mutants. (**B**) Effects of increasing amounts of 12*S* E1A on CBP-stimulated activities of the RAR (far left) and STAT1 and coactivator functions of wild-type CBP and CBPΔC/H3 molecules for the RAR and STAT1 (middle and far right). HeLa cells were transfected with a luciferase reporter gene under transcriptional control of a minimal promoter linked to two copies of the RARβ2 retinoic acid response element (RARE/Luc) or eight copies of a consensus GAS element recognized by STAT1 (GAS/Luc). Cells were cotransfected with E1A, CBP, or CBPΔC/H3 expression vectors and treated with the retinoic acid–specific ligand TTNPB, interferon-γ, or vehicle, as indicated in (*9*).

R. Kurokawa, M.-H. Ogliastro, C. K. Glass, Divisions of Cellular and Molecular Medicine and Endocrinology and Metabolism, Department of Medicine, University of California, San Diego, 9500 Gilman Drive, La Jolla, CA 92093–0651, USA.
D. Kalafus, Divisions of Cellular and Molecular Medicine and Endocrinology and Metabolism and Biomedical Sciences Graduate Program, Department of Medicine, University of California, San Diego, 9500 Gilman Drive, La Jolla, CA 92093–0651, USA.
C. Kioussi, J. Torchia, M. G. Rosenfeld, Howard Hughes Medical Institute, Department of Medicine, University of California, San Diego, 9500 Gilman Drive, La Jolla, CA 92093–0651, USA.
L. Xu, Biomedical Sciences Graduate Program, and Howard Hughes Medical Institute, Department of Medicine, University of California, San Diego, 9500 Gilman Drive, La Jolla, CA 92093–0651, USA.
*To whom correspondence should be addressed. E-mail: cglass@ucsd.edu